JOURNAL OF MATERIALS SCIENCE 32 (1997) 437–442

Effect of dynamic strain ageing on the tensile properties of a modified 9Cr–1Mo steel

R. KISHORE, R. N. SINGH, T. K. SINHA
Metallurgy Division, B.A.R.C, Trombay, Bombay 400 085, India
B. P. KASHYAP
Department of Metallurgical Engineering and Materials Science, Indian Institute of Technology, Powai, Bombay 400 076, India

Tensile testing of a modified 9Cr–1Mo steel in two microstructural conditions (710T – normalized at 1100 °C, tempered at 710 °C, and 550T – normalized at 1100 °C tempered at 550 °C) in the temperature range 25–450 °C, under strain rates of 2.3×10^{-5}–2.3×10^{-3} s^{-1}, exhibited serrated flow curves, with serrations appearing almost at the onset of deformation and disappearing before ultimate strengths were attained. The serrated flow curves (characteristics of dynamic strain ageing) were accompanied by increased ultimate strengths, loss of ductility and negative strain-rate sensitivity, relative to the ambient temperature properties. However, the increase in ultimate strength and the reduction in ductility were much larger for 710T specimens, as compared to 550T ones. In the dynamic strain ageing regime, the work-hardenability of 710T specimens increased rapidly while that of 550T specimens remained practically unaffected. Based on the microstructural consideration and the observed activation energy of 45 kJ mol^{-1}, it is proposed that serrations are initiated by a nitrogen atmosphere formation on the waiting dislocations by a pipe diffusion mechanism, and they disappear by diffusion to the precipitate sinks during deformation. Because the fine alloy carbide precipitates in 550T specimens are more effective sinks than those of 710T ones, they can cause much faster depletion of the atmosphere, resulting in a much smaller effect of dynamic strain ageing on the tensile properties of 550T specimens.

1. Introduction

It is well known that the manifestations of dynamic strain ageing in steels can occur as serrated flow curves, increased work-hardenability and ultimate tensile strength, negative strain-rate sensitivity and reduction in ductility [1, 2]. In certain applications the strengthening effects of dynamic strain ageing can be used to advantage [2, 3]. However, the ductility loss associated with this phenomenon can impair elevated temperature formability [4] of the steel sheet, and adversely affect the integrity of large components of the power industry [5]. Published data [4] on the dynamic strain ageing of a plain carbon (1008) steel, dual-phase steel and a high-strength low-alloy steel (HSLA) have shown a large decrease in ductility for the 1008 steel, whereas the ductility losses were minimal for the dual-phase and HSLA steels. The steels studied had two distinct microstructures, ferrite–martensite for dual-phase steels, and ferrite–pearlite for the plain carbon and HSLA steels. However, the dynamic strain-ageing study of a nuclear structural steel (ASTM A203 D) in tempered martensite and ferrite–pearlite microstructural conditions, did not show any significant difference in the changes in tensile strength and ductility caused by dynamic strain ageing [6].

The modified 9Cr–1Mo steel (ASTM T91) possessing an excellent combination of mechanical properties and corrosion resistance is used in power and process industries [7]. Moreover, this steel is being considered as a substitute for austenitic stainless steel in nuclear reactor systems because of its better resistance to irradiation embrittlement [8].

During routine tensile testing of a modified 9Cr–1Mo steel in tempered martensitic conditions, serrated plastic flow was observed in the range of 225–450 °C. The observed stress–strain curves were unique in the sense that the serrations appeared almost at the start of the deformation and disappeared before ultimate tensile strengths were attained. However, the occurrence of dynamic strain ageing in the range of 250–400 °C in standard 9Cr–1Mo steel in the tempered martensitic condition, has been reported to be akin to substitutional alloys, in which serrations appeared in the stress–strain curves after a critical plastic strain [9]. It was thus felt necessary to carry out a detailed analysis of the dynamic strain-ageing phenomenon, observed in the modified 9Cr–1Mo steel. In an earlier paper [10], the mechanism of the disappearance of serrations was reported. This paper deals with the mechanism of the initiation of serrations

0022–2461

on the flow curve and the effects of dynamic strain ageing (DSA) on the tensile properties of this steel in two microstructural conditions: (i) normalized (1100 °C) and tempered at 710 °C (designated 710T), (ii) normalized (1100 °C) and tempered at 550 °C (designated 550T).

2. Experimental procedure

The material used was a section of a hot-rolled billet of a modified 9Cr–1Mo steel. The chemical composition obtained by our analysis is given in Table I. Flat tensile specimens with gauge dimensions (30.0 mm $\times$ 6.35 mm $\times$ 2.0 mm) were austenitized under a helium atmosphere at 1100 °C and air cooled. Subsequently these were tempered at 550 and 710 °C. All heat-treatments (austenitization and tempering) were of 1 h duration.

The microstructure of 710T specimens (Fig. 1a) consisted of dislocated martensite laths with $Cr_{23}C_6$ precipitate (0.1 μm diameter) at lath and parent austenite boundaries. The structure of 550T specimens (Fig. 1b) showed very fine precipitate (about 0.04 μm thick) distributed predominantly within the dislocated martensite laths. Although it was not possible to identify these precipitates positively by electron diffraction, these appeared to be Cr_2C, as reported in the literature [11]. The specimens tempered at 550 °C (550T), possessed much higher hardness (VPN 455) as compared to that of 710T specimens (VPN 290) because of a secondary hardening phenomenon occurring at this temperature.

Published literature [9, 11–13] on the CCT diagram and tempering characteristics of 9Cr–1Mo class of steels, show that the normalized microstructure consists of lath martensite, auto-tempered M_3C precipitates and a high density of transformation-induced dislocations. Auto-tempering is the consequence of the relatively high martensite transformation temperature ($\sim$400 °C). The secondary hardening phenomenon occurs around 550 °C; the main contribution of the secondary hardening appears to be from M_2X precipitation at dislocations throughout the matrix. With increased heat-treatment temperatures, tempering proceeds by M_2X precipitates coarsening, decreasing dislocation density and $M_{23}C_6$ precipitation at grain and tempered lath boundaries. Transformable austenite is formed at temperatures above 875 °C only [12]. Because this class of steels contains a large amount of ferrite stabilizing elements and very little austenite stabilizing elements, no retained austenite is expected to form during hardening treatment. In the present work, the microstructural examination of as-normalized and tempered structures did not show any evidence of either transformed or retained austenite.

Tensile tests were conducted in an Instron machine at temperatures of 25 °C (ambient) to 450 °C, with nominal strain-rate varying from 2.3×10^{-5}–$2.3 \times 10^{-3}\,s^{-1}$. For elevated temperature tests, a high-temperature furnace with temperature control of $\pm$ 2 °C was used. During testing, load suppression was employed for amplifying load-drop signals associated with the serrated flow. Three specimens were tested under each temperature/strain-rate condition and an average value of the property was calculated.

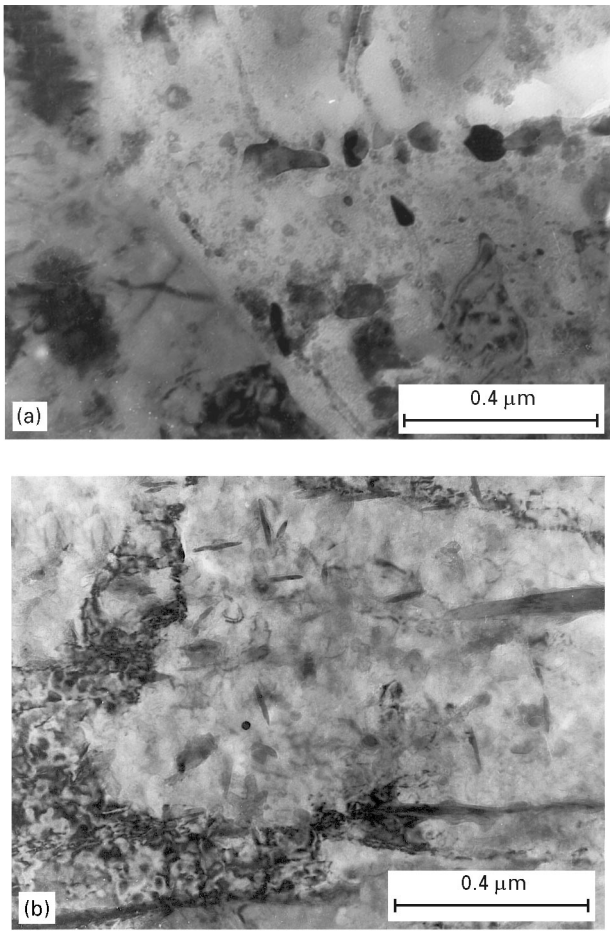

Figure 1 (a) Microstructure of 710T specimens showing large $Cr_{23}C_6$ precipitates. (b) Microstructure of 550T specimens showing fine needle-shaped precipitates (most probably Cr_2C).

3. Results

3.1. Temperature and strain-rate dependence of tensile properties

Serrated stress–strain curves were observed at 225–400 °C for 710T specimens and at 300–450 °C for 550T specimens. The main features of the stress–strain curves of both types of specimens were: (1) the appearance of very small serrations at the onset of deformation, (2) serrations becoming distinct and large in the plastic (non-linear) part of the curves, and (3) their

TABLE I The nominal composition of the steel under present investigation (wt %)

Cr	Mo	C	Si	Mn	Nb	V	P	S	N
9.5	1.0	0.1	0.5	0.35	0.08	0.21	< 0.025	< 0.025	0.025

disappearance from the flow curves before ultimate tensile strengths were attained. Typical stress–strain curves of the two types of specimens deformed at 25–450 °C with a nominal strain rate of $1.11 \times 10^{-4}\,s^{-1}$ are shown in Fig. 2a and b.

It was observed that for 710T specimens, the appearance of serrations was accompanied by an increase in work-hardening, ultimate strengths and loss of ductility. However, for the 550T specimens the values of work-hardenability and ultimate strength in the DSA range remained practically constant as did those of ambient temperature properties. It was also noted that although the 710T specimens deformed at 450 °C yielded a smooth flow curve, the high work-hardenability and ultimate strength still persisted. Further, it was found that the reduction of ductility associated with serrated flow was much larger for 710T specimens than that in 550T specimens. The changes in tensile properties of both types of specimens during dynamic strain ageing are illustrated more explicitly in Figs 3 and 4. The temperature dependence of ultimate tensile strengths for 550T and 710T specimens at two levels of strain rate (Fig. 3a) revealed that in the DSA regime the ultimate strength of both specimens increased with increase in test temperatures (with a peak around 350 °C) and decreased with increasing strain rate, indicating the negative strain-rate sensitivity. The negative strain-rate sensitivity is also demonstrated in the strain-rate dependence of flow stress at 300 °C for the two types of specimens (Fig. 3b). It is also apparent (Fig. 3a) that the increase in the ultimate strength caused by dynamic strain ageing is more pronounced for 710T specimens compared to that in 550T specimens.

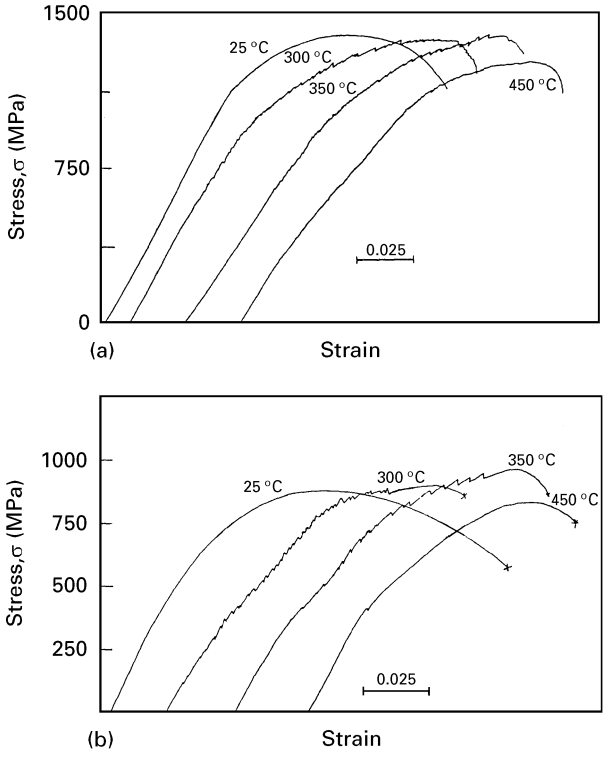

Figure 2 Typical stress–strain curves for (a) 550T and (b) 710T specimens, at a strain-rate of $1.11 \times 10^{-4}\,s^{-1}$.

Fig. 4a shows that, in the DSA region, the initial work-hardenability of 710T specimens increased rapidly with increasing temperature with a peak around 350 °C, while in the same temperature region, the work-hardening rate of 550T specimens did not show any appreciable increase over the ambient properties. The high value of work-hardening compared to that at ambient temperature persisted in 710T specimens at 450 °C, where the flow curve had become serration free (Fig. 2a). Fig. 4b shows the variation of ductility (total per cent elongation) with test temperature. It was observed that around 350–400 °C, the 710T specimens suffered a large decrease in ductility (~50%), while the decrease was very small for 550T specimens. These results clearly indicate that the effect of DSA on ductility was more severe in 710T specimens than in 550T ones.

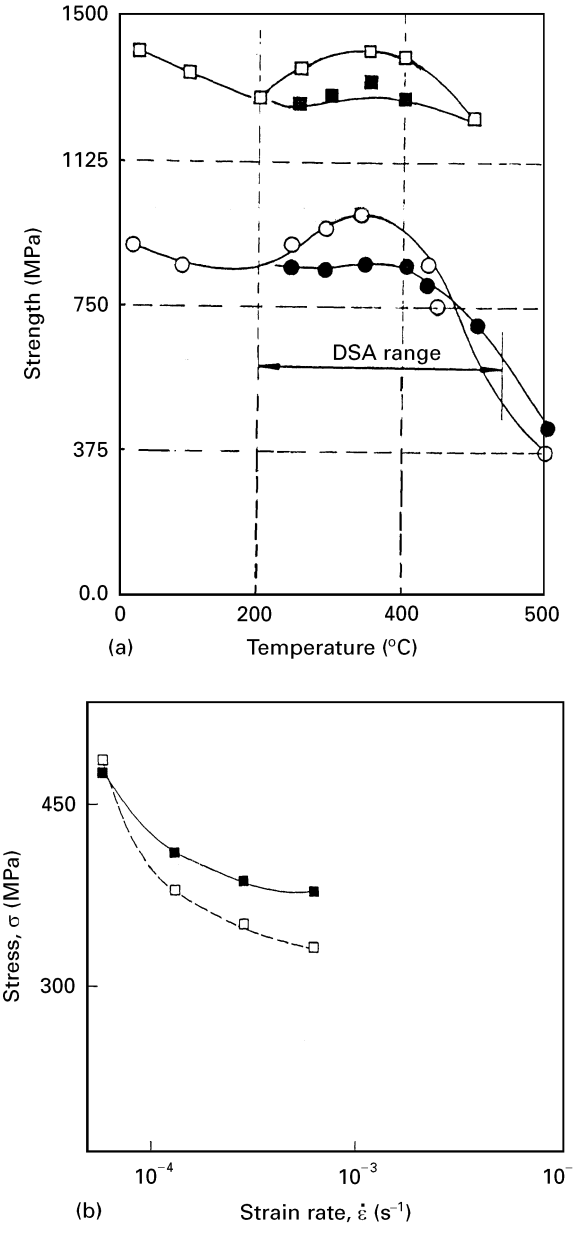

Figure 3 (a) Temperature dependence of ultimate strength for (○, ●) 710T and (□, ■) 550T treatment at the strain rates of (□, ○) 1.11×10^{-4} and (■, ●) $2.77 \times 10^{-4}\,s^{-1}$. (b) Variation of flow stress with strain-rate at $\varepsilon = 1.85\%$ (total) for (□) 710T and (■) 550T treatments at 300 °C.

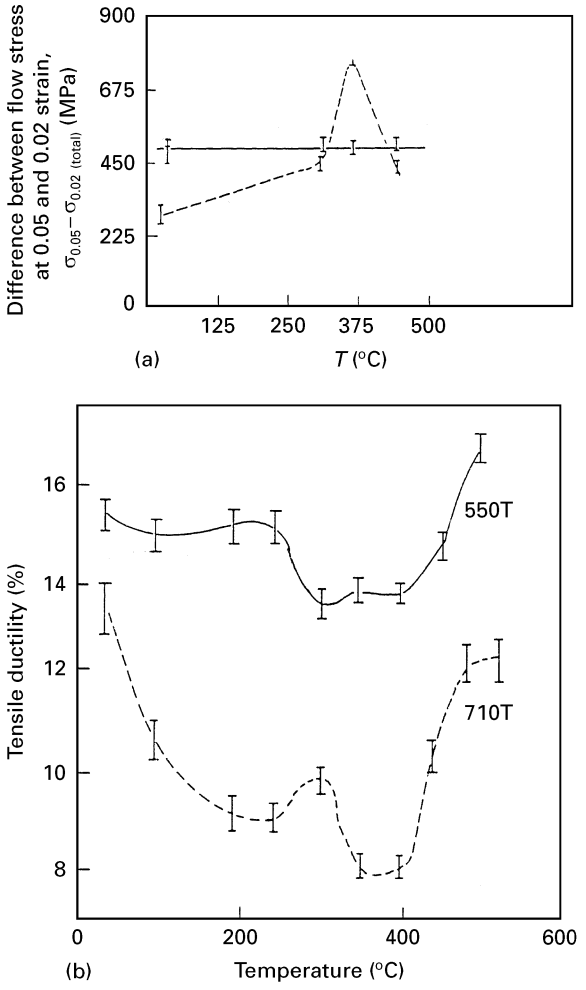

Figure 4 (a) Variation of σ (between two strain levels) with test temperature for (——) 550T and (– – –) 710T treatments, at $\dot{\varepsilon} = 1.11 \times 10^{-4}\ s^{-1}$. (b) Variation of tensile ductility at various test temperatures for (– – –) 710T and (——) 550T conditions, at $\dot{\varepsilon} = 1.11 \times 10^{-4}\ s^{-1}$.

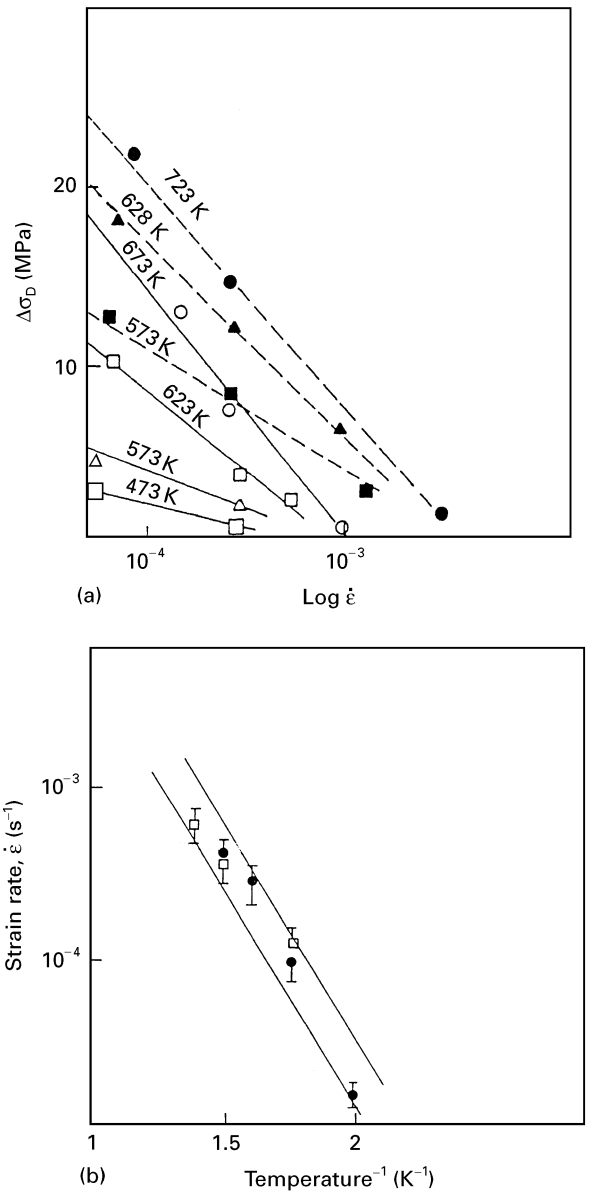

Figure 5 (a) Plot of σ_D versus log $\dot{\varepsilon}$ at constant $\varepsilon = 0.04\%$ for (– – –) 550T and (——) 710T at various test temperatures. (b) Arrhenius plot of strain-rate versus $1/T$ at constant σ_D: (●) 10 MPa, 550T; (□) 3 MPa, 710T. $Q = 45.1 \pm 8\ kJ\ mol^{-1}$.

3.2. Apparent activation energy of dynamic strain-ageing

Because the serrations appeared in the stress–strain curves of both types of specimens almost at the beginning of deformation, the activation energy could not be determined by the more conventional criterion based on measuring the critical strain or strain rate to the onset of serrations. It has been suggested by Hayes and Hayes [14, 15] that a more fundamental measurement of dislocation solute atmosphere interaction could be obtained by measuring the height of the serrations, σ_D (stress decrement) and plotting this against strain rate, $\dot{\varepsilon}$. The curves of σ_D, at a given strain value for the two types of specimens, versus log($\dot{\varepsilon}$) at various temperatures are shown in Fig. 5a. From these data the values of ΔH for the two types of specimens were obtained from the slopes of log($\dot{\varepsilon}$) at constant σ_D versus $1/T$ plots. Such plots (Fig. 5b) yielded an activation energy value of about 45.1 kJ mol^{-1} for both types of specimens studied. The observed value of ΔH is much less than those for lattice diffusion of nitrogen or carbon in α iron [16].

4. Discussion

The present studies of the modified 9Cr–1Mo steel show that the ultimate tensile strengths of both types of specimens increase with increasing temperature, reach maximum at about 350 °C and then decrease with further increase in temperature. Correspondingly, the ductility decreases with increasing temperature, reaching minimum values at around 350–400 °C, and then increases with increase in test temperatures. In 710T specimens, the rate of work-hardening increases rapidly with increasing temperature, reaching a peak around 350 °C (Fig. 4a), and then decreasing with further increase in test temperature. On the other hand, the work-hardening of 550T specimens remain practically unchanged in the test temperature range (300–450 °C), where the serrated flow curves are observed. The observed changes in tensile properties due to dynamic strain ageing in the

steel of the present investigation are similar to the well-known characteristics observed in plain carbon and alloy steels [1]. It has been shown that there is much greater increase in dislocation density for a given strain in the DSA range than at ambient temperature, giving rise to enhanced work-hardening rate. The major contributions to the increased flow or ultimate stress come from the increased work-hardenability [1]. Lou and Northwood [17] have shown in their study on elevated temperature tensile properties of a pressure vessel steel, that the degree of dynamic strain ageing can be correlated with an increase in the magnitude of work-hardening relative to that at ambient temperature.

The results of present work show that in the DSA region, the increase in the magnitude of work-hardening relative to that at ambient temperature is quite large for 710T specimens but the increase in work-hardenability compared to that at ambient temperature is negligibly small in 550T specimens in the temperature range of serrated flow. This indicates that the degree of dynamic strain ageing in 550T specimens containing very fine second-phase particles (carbide) is much smaller compared to 710T specimens containing relatively coarser carbide particles. Hayes and Hayes [15] observed the complete disappearance of serrated flow in a $2\frac{1}{4}$Cr–1Mo steel tempered in the secondary hardening condition (containing fine alloy carbide particles), while the same steel in the annealed condition exhibited serrated flow [15]. The strong influence of microstructure on the DSA behaviour of the $2\frac{1}{4}$Cr–1Mo steel was proposed to be due to the fine alloy carbides acting as extremely effective sinks depleting the interstitial (carbon) atmosphere from the dislocations [15].

The three notable observations of the present work are:

(i) a strong effect of microstructure on the changes in tensile properties (particularly the reduction in ductility) by DSA;

(ii) an apparent activation energy for the initiation of serrations much smaller than the lattice diffusion of carbon or nitrogen;

(iii) the persistence of a negative strain-rate sensitivity in 710T specimen above 400 °C, even when the curves become serration free.

These observations can be explained, at least qualitatively, with the help of a proposed model on the mechanism of serrated flow in the steel investigated. In the tempered martensitic structures of the steel of the present study, practically all carbon should be tied up as chromium carbides, resulting in negligibly small strain-ageing effect by carbon. However, the presence of a sufficient concentration of nitrogen can cause strain ageing. The proposed model is as follows.

(a) The interstitial (nitrogen) atmosphere forms on dislocations during their arrest time at obstacles, as proposed by Sleeswyk [18]. Serrations appear when the net nitrogen concentration on the dislocation exceeds the critical concentration required for the formation of sufficiently large atmosphere. The phenomenon involves the pipe diffusion of nitrogen from forest dislocations to the waiting mobile dislocations. Because the activation energy for pipe diffusion (through a dislocation) is about 0.4–0.7 of the activation energy for lattice diffusion, the observed values of activation energy for the appearance of serrations is low ($\sim 45.1\ \mathrm{kJ\,mol^{-1}}$) compared to that for lattice diffusion of nitrogen ($\sim 80\ \mathrm{kJ\,mol^{-1}}$).

(b) With increasing deformation, nitrogen drains off the arrested dislocation by diffusing to the precipitate sinks and the serrations disappear when the nitrogen concentration on the dislocations falls below the critical concentration needed to maintain the serrated flow. Because the alloy carbide precipitates present in the 550T specimens are much finer compared to those in 710T specimen, they can act as more effective sinks, causing faster depletion of the nitrogen atmosphere, thereby decreasing the degree of dynamic strain ageing. Thus, much smaller effects of DSA on the changes in tensile properties are observed in 550T specimens. The effect of serrated flow and interstitial content on ductility has been discussed extensively by Baird [1]. Sachdev [4] proposed that, during serrated flow, one of the Luder's bands could be a potential site for failure, the probability of such failure increasing as the material work-hardens. Therefore, it appears that in the temperature/strain-rate regime where DSA occurs, there is a direct correlation between the increase in work-hardening and the decrease in ductility of the material.

The relationship between the onset of serrated flow and strain-rate sensitivity has been elaborately treated by Mulford and Kocks [19] and Hayes and Hayes [15]. It has been suggested [15] that the negative strain-rate sensitivity is produced by the gradual increase in atmosphere size up to the critical size at which serrations appear on the flow curve. Further, the persistence of the negative strain-rate sensitivity after the disappearance of serrations was suggested to be a result of the precipitation reaction depleting the dislocations of their atmosphere. In the present work, the tempered martensite structures of 710T specimens are very stable in the temperature range of testing, so the persistence of the negative strain-rate sensitivity at 450 °C (when the flow curve has become serration free), cannot be due to any precipitation reaction. Lou and Northwood [17], in their study on dynamic strain-ageing in a pressure vessel steel, having ferritic–pearlitic microstructure, observed that at 250 °C, a negative strain-rate dependence of strength persisted even though there was no serrated yielding at that temperature. The latter authors suggested that, at higher temperatures and low strain-rates, the locked dislocations can drag their atmosphere with them (semi-locked condition) and serrated yielding is unlikely to occur. However, in a study on the mechanism of the disappearance of serrations in tempered martensite of this steel we have suggested the disappearance of serrations occurs by diffusion of nitrogen from dislocations to the precipitate sinks [10]. It is thus felt that more work is needed to understand clearly the mechanism controlling the persistence of negative strain-rate sensitivity during dynamic strain ageing, even at temperatures where flow curves were serration free.

5. Conclusions

1. The modified 9Cr–1Mo steel in two microstructural conditions (550T and 710T), are both susceptible to dynamic strain ageing, which leads to serrated flow. This phenomenon is associated with maxima in ultimate tensile strengths, minima in ductility and negative strain-rate sensitivity of flow stress. In the regime of dynamic strain-ageing, the increase in the rate of work-hardening and the decrease in ductility were found to be quite large for 710T specimens, while for 550T specimens, neither the increase in work-hardenability nor the loss in ductility were appreciably affected.

2. It is proposed that the initiation of serrations occurs by the formation of an interstitial (nitrogen) atmosphere on dislocations during their arrest time at obstacles. The phenomenon involves pipe diffusion through forest dislocations to the waiting dislocations with an apparent activation energy of 45.1 $kJ\,mol^{-1}$ (0.47 eV).

3. It is suggested that with increasing deformation, nitrogen drains off the arrested dislocations by diffusing to the precipitate sinks. As the alloy carbide precipitates present in the 550T specimens are much finer, compared to those in 710T specimens, they can act as more effective sinks, causing much faster depletion of the nitrogen atmosphere and thereby decreasing the degree of dynamic strain ageing. Consequently, much smaller effects of dynamic strain ageing on the changes in tensile properties are observed in 550T specimens.

4. The persistence of a negative strain-rate sensitivity in 710T specimens at 450 °C where there was no serrated yielding, cannot be adequately explained with the help of current theories of strain ageing.

References

1. J. D. BAIRD, "The Inhomogenity of Plastic Deformation" (ASM, Metals Park, OH, 1973) p. 191.
2. J. D. BAIRD, *Metal Rev.* No. 149, **5**(2) (1971) 1.
3. C. C. LI and W. C. LESLIE, *Metall Trans.* **9A** (1978) 1765.
4. A. K. SACHDEV, *ibid.* **13A** (1982) 1793.
5. B. OSTENSSON, "Reliability Problems of Reactor Pressure Vessel Components", Vol. 1 (International Atomic Energy Agency, Vienna, 1978) p. 303.
6. J. K. CHAKRAVARTTY, S. L. WADEKAR, T. K. SINHA and M. K. ASUNDI, *J. Nucl. Mater.* **11** (1983) 51.
7. A. K. KHARE (ed.), "Proceedings of the Conference on Production, Fabrication and Properties of Ferritic Steels for High Temperature Applications", (ASM, Metals Park, OH, 1983).
8. D. S. GELLES, *ISIJ Int.* **30** (1990) 905.
9. R. K. UPADHYAYA and M. N. SHETTY, *Z. Metallkde.* **82** (1991) H 1.
10. R. KISHORE, R. N. SINGH, T. K. SINHA and B. P. KASHYAP, *Scripta Metall. Mater.* **32** (1995) 1297.
11. W. B. JONES, C. R. HILLS and D. H. POLONIS, *Metall. Trans.* **22A** (1991) 1049.
12. S. J. SANDERSON, in "Proceedings of the Conference on Production, Fabrication and Properties of Ferritic Steels for High Temperature Applications", edited by A. K. Khare (ASM, Metals Park, OH, 1983) p. 85.
13. VANDER VOOT (ed.), "Atlas of Time Temperature Diagrams for Iron and Steels" (ASM, Metals Park, OH, 1991) p. 572.
14. R. W. HAYES and W. C. HAYES, *Acta. Metall* **30** (1982) 1295.
15. *Idem*, *ibid.* **32** (1984) 259.
16. A. T. STEPHENSON, *Trans. Am. Inst. Min. Eng.* **233** (1985) 1183.
17. S. LOU and D. O. NORTHWOOD, *Can Metall. Q.* **31** (1992) 225.
18. A. W. SLEESWYK, *Acta. Metall.* **6** (1958) 598.
19. R. A. MULFORD and U. F. KOCKS, *ibid.* **27** (1979) 1125.

Received 6 February
and accepted 2 July 1996